

FIRST ANALYSIS OF THE EFFECT OF THE JOVICENTRIC DECLINATION OF THE EARTH ON THE OBSERVATION OF JOVIAN DECAMETRIC RADIO EMISSIONS

H. R. P. Jácome¹, M. S. Marques², P. Zarka^{3,4}, E. Echer¹, L. Lamy^{3,4,5}
and C. K. Louis⁶

Abstract

Through analysis of the extensive catalog of the Nançay Decameter Array, from 1978 to 2020, we demonstrate that the effect of the variation of the Jovicentric declination of the Earth on the visibility of Jovian decametric radio emissions by ground-based instruments is combined with the effects of variation of the Earth-Jupiter distance and of Jupiter's elongation. Therefore, these superimposed effects must be considered and removed for the study of the pure effect of the declination on the emissions' visibility.

1 Introduction

The Jovian decametric (DAM) radio emissions are the only known type of non-thermal planetary radiation that can be detected by ground-based radio instruments because of their high frequencies, up to 40 MHz, that overcome the cut-off frequency of the terrestrial ionosphere. For this reason, the Jovian DAM emissions were the first clue of the existence of a magnetic field and magnetosphere at Jupiter, and have been continuously observed by ground-based instruments for decades. One factor that is long known to affect the visibility of the Jovian DAM emissions by ground-based instruments, besides the cut-off

¹DIHPA, CGCE, Instituto Nacional de Pesquisas Espaciais, São José dos Campos, Brazil

²Departamento de Geofísica, Universidade Federal do Rio Grande do Norte, Natal, Brazil

³LESIA, Observatoire de Paris, Université PSL, CNRS, Sorbonne Université, Université de Paris, Meudon, France

⁴Observatoire de Radioastronomie de Nançay, Observatoire de Paris, Université PSL, CNRS, Univ. Orléans, Nançay, France

⁵Aix Marseille Université, CNRS, CNES, LAM, Marseille, France

⁶School of Cosmic Physics, DIAS Dunsink Observatory, Dublin Institute for Advanced Studies, Dublin 15, Ireland

frequency of the terrestrial ionosphere limiting the minimum observed frequency, is the variation of the Jovicentric declination of the Earth (D_E), i.e., the sub-Earth Jovicentric latitude. It has been observed that, as D_E varies, the distribution of each component of the Jovian DAM emissions as a function of the longitude and of Io orbital phase changes, for instance, in amplitude and in width. This could result from the position of the radiation beaming cones (cyclotron maser instability cones (Wu & Lee, 1979)) relative to the observer that becomes more or less visible as the declination changes (Carr et al., 1970; Boudjada & Leblanc, 1992; Leblanc et al., 1993; Garcia, 1996; Imai et al., 2011, and references therein). Advances in the study of Jovian DAM radiation generation and in simulations of their visibility have improved the understanding of the observation constraints and, consequently, of the geometry of the radiation beaming cones, which are most probably oblate cones centered in Jovian magnetic field lines (Galopeau & Boudjada, 2016; Louis et al., 2017). In this context, the comprehension of the declination effect on the Jovian DAM emission visibility could contribute to validate and possibly improve the beaming cone morphology.

However, although some aspects of the effect of the variation of D_E have been observed and studied, a real and clear relation between it and the visibility of Jovian DAM emissions is still an open question that might be answered through a long-term, multidecadal study of the emissions variability with D_E . The radio observation of Jupiter by the Nançay Decameter Array (NDA) since 1978 provides an extensive database of Jovian DAM emissions (Lamy et al., 2017), which in turn allows in-depth studies of the Jovian DAM components (Zarka et al., 2017; Marques et al., 2017; Zarka et al., 2018; Jácome et al., 2022) and enables the study of their long-term variability.

A surprising behavior of the daily observations of Jupiter by the NDA and of the detected Jovian DAM emissions is that the majority of them are distributed in clusters around specific values of D_E , such as -3° , -1.5° , 0° , 2° and 3.5° , with just a relatively few cases occurring between these clusters, as shown in the histogram of Figure 1a. This type of distribution is even clearer for the emissions, which seems to indicate that the visibility of the emissions is favoured when the declination is around those values. However, more intriguing than that is the conservation of the clustered distribution when analyzing the ratio of the number of emissions to the number of observations for each bin of declination, showed in the panel *b*. It suggests that the occurrence of observations of Jupiter with no emission detection is less frequent around the declination values of -3° , -1.5° , 0° , 2° and 3.5° . The same inference may be deduced from the distribution of the emissions' occurrence probability, shown in Figure 1d. The probability was calculated from the ratio of the sum of the duration of the emissions to the sum of the duration of the observations for each 0.25° of declination. The distribution of the total duration of the emissions and of the observations found in each 0.25° bin is shown in panel *c*.

If one considers the variation of the declination in time, shown in Figure 2, it can be noted that the Earth spends more time in D_E around -3° , -1.5° , 0° , 2° and 3.5° , which could explain the higher amount of observations and detected emissions around these values. But what about the detection probability? We would expect it to present an approximately flat distribution in declination if detection depended only on the amount of time that the Earth spends around declination values more favourable to Jovian emissions'

66 observation. As we still observe a modulation vs. D_E of the occurrence probability, this
 67 means that other factors must also affect the detection of Jovian DAM emissions.

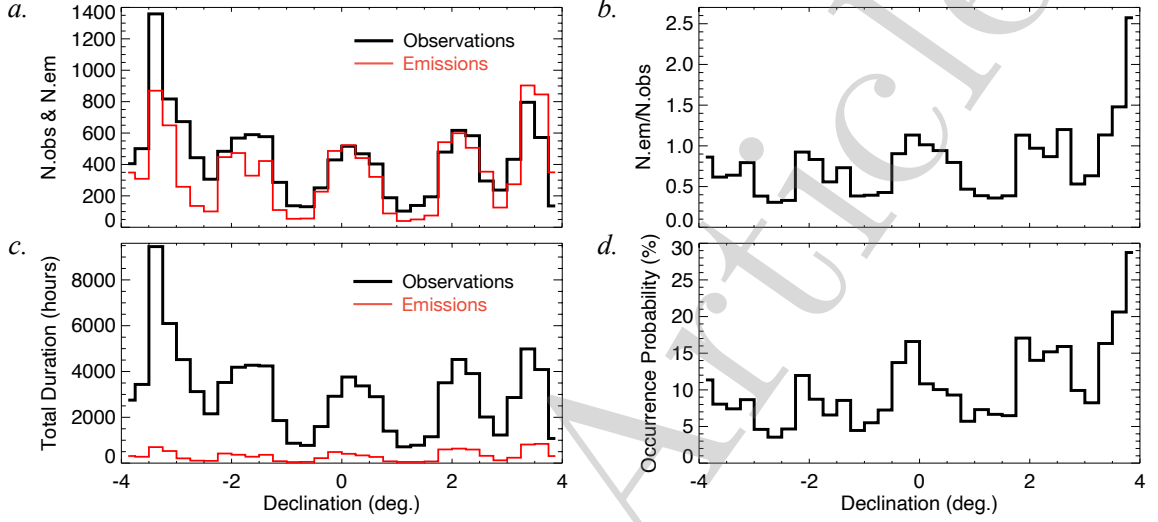


Figure 1: (a) Number of observations (black) and detected emissions (red) found in intervals of 0.25° of the jovicentric declination of the Earth. (b) Ratio of the number of emissions to the number of observations in each bin of the histogram in panel a. (c) The sum of duration, in hours, of the observations (black) and of the emissions (red) found in each 0.25° bin. (d) Emissions' occurrence probability (%), calculated from the ratio of the sum of duration of the emissions to the sum of duration of the observations for each interval of declination.

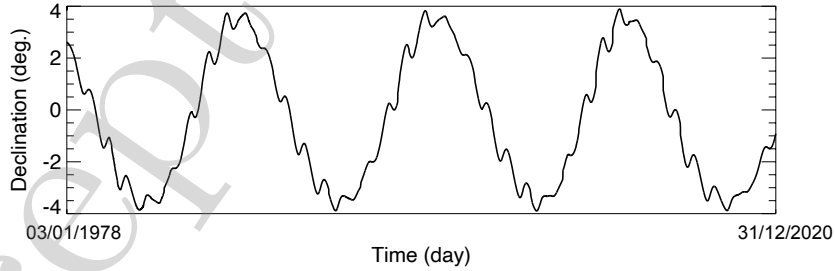


Figure 2: Daily variation of the Jovicentric declination of the Earth, from Jan. 3th, 1978 to Dec. 31st, 2020.

68 In this work, we identify two other factors of the relative motion between the Earth and
 69 Jupiter that also affect the visibility of the Jovian DAM emissions and are combined
 70 with the D_E effect: the variation of the distance between the Earth and Jupiter and the
 71 variation of Jupiter's elongation, both sketched in Figure 3.

72 2 Method

73 We use the extensive digital catalog of the NDA, which comprises all the observations of
 74 Jupiter by the array from January 3, 1978 to December 31, 2020, with all the detected

emissions in this period (Lamy et al., 2017; Marques et al., 2017). We have plotted the distributions of all the observations of Jupiter by the NDA, all the Jovian DAM emissions catalogued and the occurrence probability of the emissions as a function of D_E versus the Earth-Jupiter distance (Figure 4) and of D_E versus Jupiter’s elongation (Figure 5).

The Earth-Jupiter distance, which varies from ~ 4.0 AU to 6.5 AU, can affect the intensity of the detected emissions, with the less intense ones being detected only at shortest distances. Jupiter’s elongation affects the minimum frequency of the detected emissions, with emissions with lower frequency (e.g., freq. < 25 MHz) being detected only when the planets are close to opposition (i.e., when Jupiter is observed in the Earth’s night-side sky), due to the increased radio interference in the day side that limit the visibility of low frequencies.

Figure 3 shows a sketch of the Earth and Jupiter and the distance (R) and Jupiter’s elongation (θ). R is the distance between the planets at the meridian transit of Jupiter for each observation, given in the NDA catalog. θ is the angle between the Sun and Jupiter, observed from the Earth, with $\theta \rightarrow 0^\circ$ indicating that the planets are close to conjunction; and $\theta \rightarrow \pm 180^\circ$, that the planets are close to opposition. Jupiter’s elongation was collected for each day from January 1st, 1978 to December 31, 2020, from NASA’s Horizons System¹.

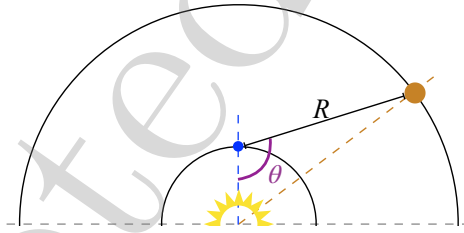


Figure 3: Sketch (not to scale) of the Earth (in blue) and Jupiter (in orange) on their orbits, with the distance (R) and Jupiter’s elongation (θ). When $\theta = 0^\circ$, the planets are in conjunction, and when $\theta = \pm 180^\circ$, they are in opposition.

3 Results

Figure 4 shows distributions of all the observations of Jupiter by the NDA, from 1978 to 2020 (panel *a*), of all the detected Jovian DAM emissions (panel *b*) and of the occurrence probability of those emissions (panel *c*) as a function of D_E and of the Earth-Jupiter distance. It is observed that, for distances shorter than 5.5 AU, the observations occur around D_E values of -3° , -1.5° , 0° , 2° and 3.5° , which explains why the majority of the observations accumulate around those values. However, for longer distances, observations occur over the entire D_E range. We also note that the observations are quite homogeneously distributed in distance, with only a smooth increase in number (panel *a*) around the shortest (~ 4.25 AU) and the longest (~ 6.25 AU) distances.

¹<https://ssd.jpl.nasa.gov/horizons/app.html>

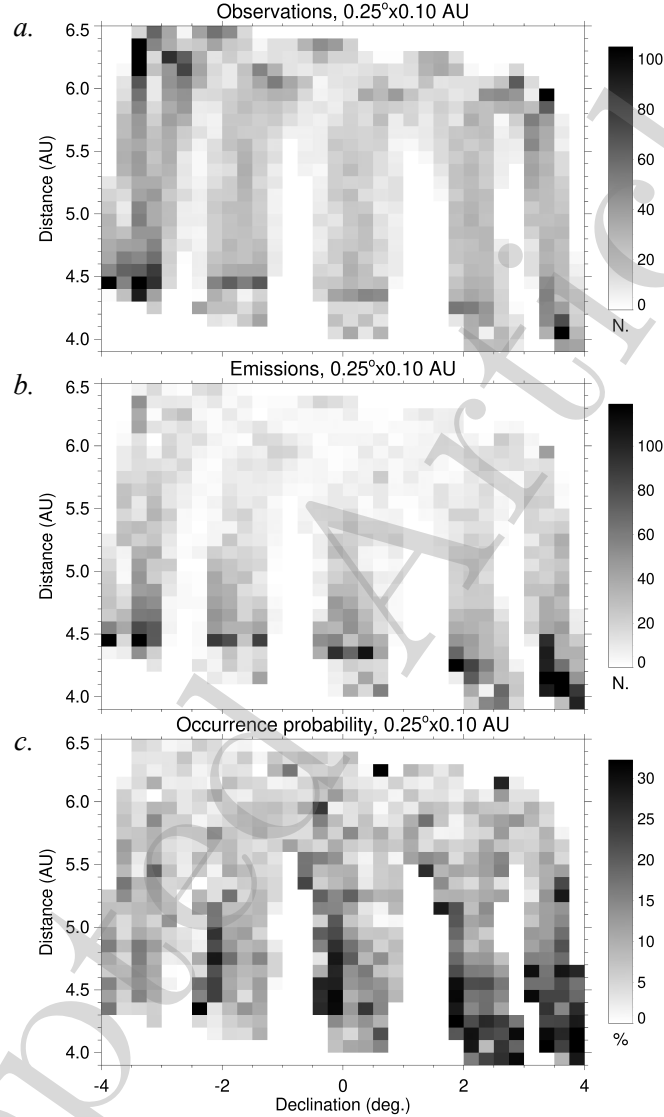


Figure 4: Distributions of all the observations of Jupiter (a) by the Nançay Decameter Array, from 1978 to 2020; of all the detected Jovian DAM emissions (b); and of the emissions' occurrence probability (c), as a function of the jovicentric declination of the Earth and of the Earth-Jupiter distance.

103 The distribution of the emissions (panel b of Figure 4), on the other hand, shows that
 104 although emissions are detected over the entire distance range, they accumulate at the
 105 shortest distances, which indicates that the emissions detection is favoured by the shortest
 106 distance between the Earth and Jupiter. As a consequence, the emissions' occurrence
 107 probability (panel c) is higher at the shortest distances, as observed in Figure 1.

108 In summary, although Jupiter is observed by the NDA over the entire Earth-Jupiter
 109 distance range, most of the emissions are detected when this distance is shortest, which
 110 always coincides with D_E values around -3° , -1.5° , 0° , 2° and 3.5° .

111 Figure 5 shows distributions of all the observations of Jupiter by the NDA, from 1978 to
 112 2020 (panel a), of all the detected Jovian DAM emissions (panel b) and of the occurrence

113 probability of those emissions (panel *c*) as a function of D_E and of Jupiter's elongation. In
 114 panel *a*, we see that the observations are homogeneously distributed over the entire range
 115 of the elongation angle. The emissions visibility (panel *b*), however, is favoured when the
 116 planets are close to opposition ($\theta \rightarrow \pm 180^\circ$). Otherwise, only a few emissions are detected,
 117 most probably the ones with the highest frequencies. As the planets opposition coincides
 118 with D_E values around -3° , -1.5° , 0° , 2° and 3.5° , this explains why the emissions and
 119 their higher occurrence probability accumulate around those values.

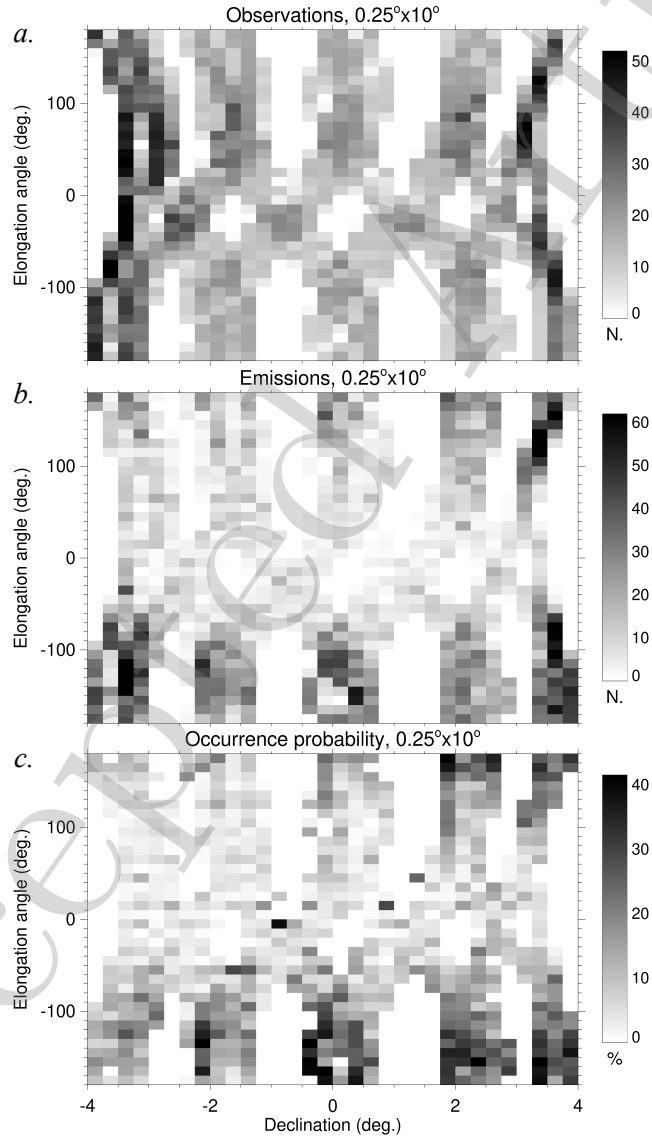


Figure 5: Distributions of all the observations of Jupiter (*a*) by the Nançay Decameter Array, from 1978 to 2020; of all the detected Jovian DAM emissions (*b*); and of the emissions' occurrence probability (*c*), as a function of the joventric declination of the Earth and of Jupiter's elongation.

120 In summary, although Jupiter is observed by the NDA over the entire range of the planet's
 121 elongation, most of the emissions are detected when it is around opposition with the Earth,
 122 which always coincides with D_E values around -3° , -1.5° , 0° , 2° and 3.5° .

123 4 Conclusions and Perspectives

124 We have presented an initial analysis of the effect of the variation of Jovicentric declination
 125 of the Earth on the detection of Jovian DAM emissions by ground-based instruments such
 126 as the Nançay Decameter Array. We have demonstrated that the detection of emissions is
 127 favoured when the planets are close to opposition ($\theta \rightarrow \pm 180^\circ$) and the distance between
 128 the planets is smallest (less than 5.5 AU), which both coincide with D_E around -3° ,
 129 -1.5° , 0° , 2° and 3.5° . Therefore, the D_E effect is actually combined with the effect of
 130 the variation of the distance and of Jupiter's elongation. Our first conclusion is that the
 131 results of all past studies of the D_E effect (e.g. Barrow (1981)) are unreliable because
 132 the effects of the Earth-Jupiter distance and of Jupiter's elongation associated with it
 133 were not identified and thus not corrected. In order to study and understand the real
 134 declination effect, those other superimposed effects must be removed by adequate data
 135 selections.

136 For the next step, we intend to remove the effect of the distance and of Jupiter's elongation
 137 by selecting emissions whose observation is not limited by distance or radio interference,
 138 i.e., emissions that can be detected over the entire ranges of Earth-Jupiter distance (~ 4 –
 139 6.5 AU) and of Jupiter's elongation (from opposition to conjunction). Then, we will study
 140 the pure D_E effect on the Jovian DAM emissions visibility.

141 The results will be compared to simulations of the emissions' dynamic spectra, with
 142 ExPRES (Louis et al., 2019), in order to interpret them.

143 5 Acknowledgements

144 This study was financed in part by the Coordenação de Aperfeiçoamento de Pessoal de
 145 Nível Superior - Brasil (CAPES) - Finance Code 001. E. Echer would like to thank
 146 the Brazilian agencies CNPq (PQ-301883/2019-0) and FAPESP (2018/21657-1) for the
 147 research grants. C. K. Louis' work at DIAS is supported by the Science Foundation Ireland
 148 Grant 18/FRL/6199. The authors thank the Brazilian Ministry of Science, Technology
 149 and Innovation and the Brazilian Space Agency. The French co-authors acknowledge
 150 support from CNES and CNRS/INSU programs of planetology (PNP) and heliophysics
 151 (PNST).

152 References

- 153 Barrow C. H., 1981, Latitudinal beaming and local time effects in the decametre-wave
 154 radiation from Jupiter observed at the Earth and from Voyager, *Astronomy and Astro-*
 155 *physics*, 101, 142
- 156 Boudjada M. Y., Leblanc Y., 1992, The variability of Jovian decametric radiation from
 157 1978 to 1988, *Advances in Space Research*, 12, 95
- 158 Carr T. D., Smith A. G., Donovan F. F., Register H. I., 1970, The twelve-year periodicities
 159 of the decametric radiation of Jupiter, *Radio Science*, 5, 495

- 160 Galopeau P. H. M., Boudjada M. Y., 2016, An oblate beaming cone for Io-controlled
161 Jovian decameter emission, *Journal of Geophysical Research: Space Physics*, 121, 3120
- 162 Garcia L. N., 1996, Long-term periodicities in the Jovian decametric emission, *PhD thesis*,
163 *University of Florida*
- 164 Imai K., Garcia L., Reyes F., Imai M., Thieman J. R., 2011, A model of Jupiter's deca-
165 metric radio emissions as a searchlight beam, *Planetary, Solar and Heliospheric Radio*
166 *Emissions (PRE VII)*, pp 179–186
- 167 Jácome H. R. P., Marques M. S., Zarka P., Echer E., Lamy L., Louis C. K., 2022, Search
168 for jovian decametric emission induced by Europa on the extensive Nançay decameter
169 array catalog, *Astronomy & Astrophysics*, 665, A67
- 170 Lamy L., Zarka Z., Cecconi B., Klein L., Masson S., Denis L., Coffre A., Viou C., 2017, in
171 eds Fischer G., Mann G., Pachenko M., Zarka P., , , *Planetary Radio Emissions VIII*.
172 *Austrian Academy of Sciences Press, Vienna*, p. 445
- 173 Leblanc Y., Gerbault A., Denis L., Lecacheux A., 1993, A catalogue of Jovian decametric
174 radio observations from January 1988 to December 1990, *Astronomy and Astrophysics*
175 *Supplement Series*, 98, 529
- 176 Louis C. K., et al., 2017, Io-Jupiter decametric arcs observed by Juno/Waves compared
177 to ExPRES simulations, *Geophysical Research Letters*, 44, 9225
- 178 Louis C. K., Hess S. L. G., Cecconi B., Zarka P., Lamy L., Aicardi S., Loh A., 2019,
179 ExPRES: an Exoplanetary and Planetary Radio Emissions Simulator, *Astronomy &*
180 *Astrophysics*, 627, A30
- 181 Marques M. S., Zarka P., Echer E., Ryabov V. B., Alves M. V., Denis L., Coffre A., 2017,
182 Statistical analysis of 26 yr of observations of decametric radio emissions from Jupiter,
183 *Astronomy & Astrophysics*, 604, A17
- 184 Wu C., Lee L., 1979, A theory of the terrestrial kilometric radiation, *The Astrophysical*
185 *Journal*, 230, 621
- 186 Zarka P., Marques M. S., Louis C. K., Ryabov V. B., Lamy L., Echer E., Cecconi B.,
187 2017, in eds Fischer G., Mann G., Pachenko M., Zarka P., , , *Planetary radio emissions*
188 *VIII. Austrian Academy of Sciences Press, Vienna*, pp 45–58
- 189 Zarka P., Marques M. S., Louis C. K., Ryabov V. B., Lamy L., Echer E., Cecconi B., 2018,
190 Jupiter radio emission induced by Ganymede and consequences for the radio detection
191 of exoplanets, *Astronomy & Astrophysics*, 618, A84